JOURNAL OF GUIDANCE, CONTROL, AND DYNAMICS
Vol. 34, No. 3, May–June 2011

Libration Synchronization Control of Clustered Electrodynamic Tether System Using Kuramoto Model

Hirohisa Kojima* and Hiroki Iwashima†
Tokyo Metropolitan University, Hino, Tokyo 191-0065, Japan
and
Pavel M. Trivailo‡
Royal Melbourne Institute of Technology, Melbourne, VIC 3083, Australia

DOI: 10.2514/1.52410

This paper proposes a new configuration for a tethered satellite system, named the "clustered electrodynamic tether system." This configuration consists of multi-electrodynamic tethered satellite systems located in a record disk orbit, which is a useful orbit for formation flight of multisatellite. The main difference of the clustered electrodynamic tether system from usual constellation flight configurations is that the clustered electrodynamic tether system uses tethers. This new configuration, thus, can be interpreted as constellation flight both toward out-of-plane direction using a record disk orbit, and in-plane direction using tethers. If librational motion of the clustered electrodynamic tether system is synchronized, the clustered electrodynamic tether system can serve as a platform system to periodically capture launched payloads and to move them to higher altitude, or a system to periodically observe the atmosphere at different altitudes at the same time. To synchronize the librational motion of the clustered electrodynamic tether system, control methods based on the Kuramoto model are proposed. The Kuramoto model is a mathematical model that can be used to describe synchronized behavior of a large set of coupled oscillators. In this paper, the proposed control methods are validated by numerical simulations.

Nomenclature

a	=	major axis, km
$\hat{a}$, $\hat{b}$	=	minor and major radius of the record disk orbit projected on the x-y plane of the Hill's coordinate, respectively, km
$\boldsymbol{B}$	=	Earth magnetic field vector, T
C_x, C_z	=	Direct cosine matrix around the x, and z axis, respectively
e	=	eccentricity
$\boldsymbol{f}$	=	the equations of motion for the clustered electrodynamic tether systems
$\bar{\boldsymbol{f}}$	=	the equations of motion of the total system associated with $\bar{\boldsymbol{x}}$
$Gxyz$	=	orbital frame
h	=	specific angular momentum, $h = \sqrt{\mu a(1-e)(1+e)}$, m^2/s
$\boldsymbol{h}_j$	=	orbital vector of the jth tethered satellite system
I	=	electric current on the tehter, A
I_s	=	moment of inertia of each tethered system around the center of mass, $\mathrm{kg\,m}^2$
i	=	inclination, rad
$\boldsymbol{i}$, $\boldsymbol{j}$, $\boldsymbol{k}$	=	unit vectors along the Gx, Gy, and Gz, respectively
K	=	control gain for the Kuramoto model-based control
K_{dfc}	=	congrol gain for delayed feedback control
L	=	length of tether, km
ℓ	=	distance along the tether from the subsatellite, km
$\hat{\boldsymbol{l}}$	=	unit vector along the tether in the orbital frame
$\boldsymbol{M}(\tau)$	=	monodromy matrix
m	=	mass of the system $= m_1 + m_2$, kg
m_1, m_2	=	mass of the mother satellite, and subsatellite, respectively, kg
N	=	the number of the tethered systems on the record disk orbit $= 3$
$\boldsymbol{p}_{cm_j}$	=	position of the mass center of the jth tethered satellite system in the inertia frame
r	=	orbital radius, km
$\boldsymbol{r}_{p_j}$	=	periapsis direction vector of the jth tethered satellite system
$\boldsymbol{T}_e$	=	torque induced by the electrodynamic force, Nm
$\boldsymbol{T}_G$	=	gravity gradient torque, Nm
$\boldsymbol{x}$	=	state variables of the clustered electrodynamic tether system
$\bar{\boldsymbol{x}}$	=	vector of tether angles and angular velocities, $\bar{\boldsymbol{x}} = [\theta_1, \phi_1, \dot{\theta}_1, \dot{\phi}_1, \theta_2, \phi_2, \dot{\theta}_2, \dot{\phi}_2, \theta_3, \phi_3, \dot{\theta}_3, \dot{\phi}_3]^T$
(x, y, z)	=	satellite position in the Hill's reference frame
(x_c, y_c)	=	center of the record disk orbit in the x-y plane of the Hill's coordinate, km
α	=	bias phase argument $= 2\pi/3$ rad
$\boldsymbol{\varepsilon}$	=	the control inputs vector, $\boldsymbol{\varepsilon} = [\varepsilon_1, \varepsilon_2, \varepsilon_3]^T$
ε_j	=	electrodynamic parameter for the jth electrodynamic tethered system
η	=	true anomaly, rad
θ	=	in-plane tether angle, rad
$\theta_{\max}$, $\dot{\theta}_{\max}$	=	maximum value of the in-plane angle and in-plane angular velocity of the periodic motion
$\lvert\lambda\rvert$	=	modulus of eigenvalue of the monodromy matrix
μ	=	Earth gravity constant $= 3.98613 \times 10^5\ \mathrm{km}^3/\mathrm{s}^2$
μ_m	=	intensity of the Earth magnetic dipole $= 8.1 \times 10^6\ \mathrm{T\,km}^3$
ν_j	=	angular velocity of the jth system in a Kuramoto model system, rad/s
ξ_{1i}, ξ_{2i}	=	phase argument of the ith tethered system for the Kuramoto model-based controllers 1 and 2, respectively, rad

Presented as Paper 2010-8350 at the AIAA Guidance, Navigation, and Control Conference, Toronto, Ontario, 2–5 August 2010; received 16 September 2010; revision received 2 December 2010; accepted for publication 19 January 2011.

*Professor, Department of Aerospace Engineering; hkojima@sd.tmu.ac.jp. Senior Member AIAA.

†Graduate Student, Department of Aerospace Engineering; iwashima-hiroki@sd.tmu.ac.jp.

‡Professor, School of Aerospace, Mechanical and Manufacturing Engineering; pavel.trivailo@rmit.edu.au.

ϖ = argument of the perigee, rad
ρ = mass ratio $= m_2/m$
σ = radius of the record disk, km
τ = delayed-time for a delayed feedback control, s
ϕ = out-of-plane tether angle, rad
$\phi_{\max}, \dot{\phi}_{\max}$ = maximum value of the out-of-plane angle and out-of-plane angular velocity of the periodic motion
ψ = inclination of a record disk plane from the orbital plane of the virtual satellite $= \pi/3$ rad
Ω_j = longitude of the ascending node of jth tethered satellite system, rad
ω = orbital rate, rad/s
$()'$ = differential operation with respect to true anomaly

I. Introduction

THE formation flight of multiple small satellites, which can synthesize the functionality of virtual large satellite, offers great promise for future space exploration. Because it has advantages, such as ease of keeping and changing the mission configuration by replacing a malfunctioning satellite with a new one, many missions have been proposed for the formation flight, such as "Laser Interferometer Space Antenna," or LISA [1]. The details of the parameters of the formation flight are summarized in [2,3].

A special configuration of the formation flight is known as a "record disk orbit" flight. In this configuration, the relative motion of multiple satellites is seen as a flight around the center of the so-called record disk plane at the same rate as the orbital rate, which implies that the satellites are at almost the same altitude.

Tethered satellite systems (TSS) are one of the formation flight configurations. The electrodynamic tether (EDT) systems, which are particular cases of the TSS, are expected to enable many future space missions such as reboosting of satellites, deorbiting space debris, and so on [4]. To fully understand the nature of the tethered satellite systems, and to propose new applications of tethered systems, the dynamics and control of the librational motion of nonelectro and electrodynamic tether systems have been investigated in numerous papers.

The librational motion of a constant length dumbbell model in elliptic orbits was first studied by Schechter [5]. The stability of the librations of gravity gradient satellites was studied by Modi and Brereton [6] and Brereton and Modi [7,8]. Swan [9] found that the in-plane librational motion of a tether system is driven by the magnitude of the orbit eccentricity and showed that the motion begins tumbling at an eccentricity of 0.355. Kumar and Kumar [10] studied open-loop librational control for tethers in elliptic orbits. Fujii and Ichiki [11] studied the effect of eccentricity and tether elasticity on the motion of a tethered system during station-keeping using Poincaré maps, bifurcation diagrams, and Lyapunov exponents. Fujii et al. [12] also showed that the chaotic librational motion of a tethered satellite in elliptic orbits can be made periodic by employing a delayed feedback control [13], assuming actuators via thrusters. Takeichi et al. [14] studied the effect of atmospheric drag on a three-dimensional librations of single or multiple tethered systems. Takeichi et al. [15,16] also considered a control of the librational motion of a tethered system in an elliptic orbit using periodic inputs via thrusters and deployment and retrieval. Kojima et al. [17,18] applied decoupled control methods combined with delayed feedback control to stabilize a three-mass tethered satellite system in an elliptic orbit with low eccentricity. Kojima and Sugimoto [19] showed that the odd number condition [20] exists for the in-plane librational motion of a three-mass tethered system in inclined elliptic orbits with high eccentricity by analyzing the moduli of eigenvalues of the monodromy matrix of motion, and also have proposed switching delayed feedback control to stabilize a chaotic librational motion of EDT in inclined elliptic orbits to periodic motions [21]. Peláez et al. [22], Peláez and Lara [23], Peláez and Lorenzini [24], and Peláez and Andres [25] studied periodic solutions and the delayed feedback control for EDT systems in inclined orbits. Williams presented a librational control for a tethered system in elliptic orbits with high eccentricity using a periodically changed tether length obtained by a linear receding horizon tracking controller [26], and proposed a librational control for a flexible tether using electromagnetic force and a movable attachment [27]. He also presented the periodic solution under forced current variations [28,29], proposed the energy rate control feedback [30], and the time-delayed predictive control [31] for the librations of an electrodynamic tether system. Iñarrea and Peláez [32] have applied an extended delayed feedback control to libration of electrodynamics tether system.

Contrary to the usual formation flight through multiple satellites without tethers, the altitude of satellites in TSS can be varied considerably by deploying long tethers. However, the papers cited above have treated traditional configurations of TSS, that is, only two satellites connected with each other through a tether. To extend the possibility of TSS, it is desired to introduce more sophisticated configurations. Recently, Pizarro–Chong and Misra [33] have proposed a hub-and-spoke tether configuration, Zhaoa and Cai [34] have proposed a new tethered system on a Halo orbit, and Chung [35] has proposed a decentralized nonlinear control framework for spinning tethered formation flying arrays and validated its effectiveness using the tethered formation flying testbed. These tethered systems are spinning tethered systems in which the formation flight is kept by the balance of the centrifugal force and tether tension.

The traditional gravity gradient stabilized tethered systems can be regarded as an in-plane formation flight incapable of out-of-plane formation, while a record disk orbit can be regarded as an out-of-plane formation flight, but has difficulty in carrying out out-of-plane formation with considerable altitude difference.

In this paper, we propose a new configuration of the electrodynamic tethered system, called the "clustered electrodynamic tether system," or CEDTS, which keeps multiple electrodynamic tether systems constrained to a "record disk" orbit. Because this configuration inherits advantages from the formation flight satellites set on a record disk orbit, and gravity gradient stabilized tethered systems, it can be regarded as a formation flight configuration both toward in-plane and out-of-plane direction, and thus, it can offer new future missions such as observation of high altitude atmosphere at different points at a constant interval. If the librational motion of CEDTS is synchronized with each other, the system can serve as a sky hook to periodically pick up launched payloads, or to periodically observe the atmosphere at different altitudes at the same time, and so on.

As mentioned above, librational motion of electrodynamics tethered system was often controlled by delayed feedback control. However, delayed feedback control (DFC) cannot be directly applied to CEDTS. This is because the CEDTS consists of multiple electrodynamic tethered subsystems, and even if the librational motion of each of the EDT subsystems is controlled by DFC, it does not guarantee the stability of the whole CEDTS systems. Besides, DFC requires past data to determine the control input. This requirement would be undesired for spacecraft whose memory size is not so large to record the past data for the DFC.

To overcome this problem, instead of DFC, we propose two control methods based on the Kuramoto model [36]. Because the Kuramoto model is a mathematical model that can be used to describe synchronized behavior of a large set of coupled oscillators, and it does not need past data, but refers to the phase difference among systems to determine the control input, it is desired to synchronize the librational motion of CEDTS. In this paper, stability of the proposed control methods is analyzed with respect to the control gain for the Kuramoto model, and then numerical simulations are carried out to validate the proposed control schemes.

The remainder of this paper is organized as follows: in Sec II, configuration of CEDTS is described, where conditions for a record disk orbit, on which the multiple tethered satellite systems are constrained, the Earth magnetic field model, and the multiple tethered system CEDTS are explained. In Sec III, control methods based on the Kuramoto model are proposed to synchronize the librational motion of CEDTS. In Sec IV, stability of the proposed control methods are analyzed with respect to the control gains, and the results of numerical simulations are shown to prove the validity of the proposed control schemes. Finally, the conclusion of this paper is given in Sec V.

II. Clustered Electrodynamic Tether System

A. Tether System

We assume that the center of mass of the system follows an unperturbed Keplerian inclined elliptic orbit. In this case, the orbital radius is given by

$$r = \frac{a(1-e^2)}{1+e\cos\eta} \tag{1}$$

In this study, the electrodynamic tether system is assumed to be a dumbbell model, as shown in Fig. 1. This system consists of a mother satellite, subsatellite, and tether. The mother satellite and subsatellite are labeled 1 and 2, and are assumed as particle masses, m_1, and m_2, respectively. The tether is assumed to be conductive, rigid body without mass and moment of inertia, but with length L. The moment of inertia of the system around the center of mass of the system is given by

$$I_s = m\rho(1-\rho)L^2 \tag{2}$$

Let $Gxyz$ be an orbital frame whose origin is located at the center of mass of the system, the Gx axis along the local vertical pointing to zenith and Gz axis normal to the orbital plane, and Gy axis be a cross product of Gz and Gx, as shown in Fig. 1. The in-plane and out-of-plane angles θ and ϕ are considered as the state variables. The unit vector along the tether in the orbital frame is given by

$$\hat{\boldsymbol{l}} = \cos\theta\cos\phi\boldsymbol{i} + \sin\theta\cos\phi\boldsymbol{j} + \sin\phi\boldsymbol{k} \tag{3}$$

To simplify the analysis, only gravity and Lorentz force are treated as the external forces affecting the attitude dynamics of the tethered satellite system. The gravity gradient torque is given by

$$\boldsymbol{T}_G \approx \frac{3\mu}{r^3} I_s(\hat{\boldsymbol{l}}\times\boldsymbol{i})(\boldsymbol{l}\cdot\boldsymbol{i}) = \frac{3\mu}{r^3} I_s(\sin\phi\cos\phi\cos\theta\boldsymbol{j} - \cos^2\phi\sin\theta\cos\theta\boldsymbol{k}) \tag{4}$$

To calculate the Lorentz torque affecting the EDT system, it is necessary to model the magnetic field. In this study, a nontilted dipole model, as shown in Fig. 2, is used to describe the Earth's magnetic field. Assuming the origin of the geocentric inertia frame is the center of the mass of the Earth, the magnetic field is given by using the orbital elements shown in Fig. 3 as follows:

$$\boldsymbol{B} = \frac{\mu_m}{r^3}\begin{pmatrix} -2\sin i\sin(\varpi+\eta) \\ -\cos i \\ \sin i\cos(\varpi+\eta)\end{pmatrix} \tag{5}$$

In this paper, it is assumed that the magnetic field is constant along the tether and equal to that of the center of the mass of the tethered system, and that the electric current is a time-varying parameter, but is constant along the tether. In this case, the torque induced by the electrodynamic force is obtained as

$$\boldsymbol{T}_e = \hat{\boldsymbol{l}}\times(\hat{\boldsymbol{l}}\times\boldsymbol{B})J_1 \tag{6}$$

where

$$J_1 = \int_0^L (\ell-\rho L)I\,\mathrm{d}\ell \tag{7}$$

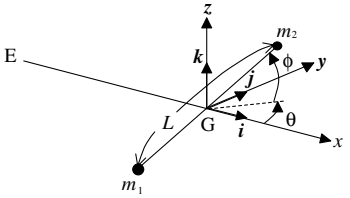

Fig. 1 Dumbbell-modeled tethered system, orbital frame and the definition of tether librational angles.

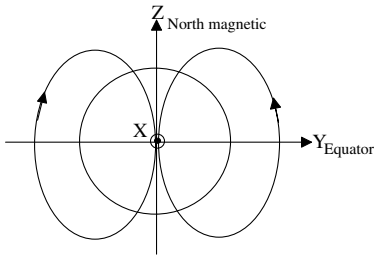

Fig. 2 Nontilted dipole model.

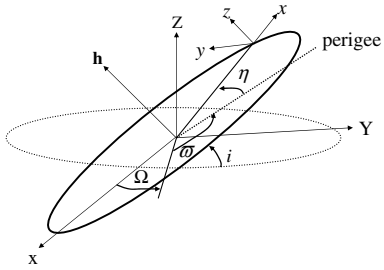

Fig. 3 Orbital elements.

We assumed that both positive and negative electric currents can be applied to the system. This means that the tether in this study is insulated and an electron collector and a plasma contactor need to be present at both ends of the tether. These assumptions will have to be removed if the bare tether is used for EDT systems, because the electric current distribution is not constant on the tether and the presence of an electron collector and a plasma contactor at both ends of the tether leads to increase of weight.

The electrodynamic parameter ε, which expresses the ratio between the electrodynamic torque and gravity gradient torque, is introduced as

$$\varepsilon = (J_1/I_s)(\mu_m/\mu) \tag{8}$$

Under assumption Eq. (1), and replacing the independent variable time t with the true anomaly η using the following relations:

$$\frac{\mathrm{d}(\,)}{\mathrm{d}t} = \frac{\mathrm{d}(\,)}{\mathrm{d}\eta}\frac{\mathrm{d}\eta}{\mathrm{d}t} = \frac{h}{r^2}(\,)' \tag{9}$$

$$\frac{\mathrm{d}\eta}{\mathrm{d}t} = \frac{\mu^2(1+e\cos\eta)^2}{h^3} \tag{10}$$

$$\frac{\mathrm{d}^2\eta}{\mathrm{d}t^2} = \frac{-2e\mu^4(1+e\cos\eta)^3\sin\eta}{h^6} \tag{11}$$

the equations of motion are obtained as follows [25]:

$$\theta'' - 2\phi'\tan\phi(\theta'+1) + 3\sin\theta\cos\theta = e[2h_1(e,\eta)(\theta'+1) + 3h_2(e,\eta)\sin\theta\cos\theta] - \varepsilon[\tan\phi\sin i\{2g_1(e,\varpi,\eta)\cos\theta - g_2(e,\varpi,\eta)\sin\theta\} + g_3(e,\eta)\cos i] \tag{12}$$

$$\phi'' + [(\theta'+1)^2 + 3\cos^2\theta]\sin\phi\cos\phi = e[2h_1(e,\eta)\phi' + 3h_2(e,\eta)\sin\phi\cos\phi\cos^2\theta] + \varepsilon\sin i[2g_1(e,\varpi,\eta)\sin\theta + g_2(e,\varpi,\eta)\cos\theta] \tag{13}$$

where h_1, h_2, g_1, g_2, and g_3 are functions given by

$$h_1(e,\eta) = \frac{\sin\eta}{1+e\cos\eta} \tag{14}$$

$$h_2(e,\eta) = \frac{\cos\eta}{1+e\cos\eta} \tag{15}$$

$$g_1(e,\varpi,\eta) = \frac{\sin(\varpi+\eta)}{1+e\cos\eta} \tag{16}$$

$$g_2(e,\varpi,\eta) = \frac{\cos(\varpi+\eta)}{1+e\cos\eta} \tag{17}$$

$$g_3(e,\eta) = \frac{1}{1+e\cos\eta} \tag{18}$$

In this study, the electrodynamic parameter ε is treated as the control input, and the tether angles θ and ϕ are treated as the output variables, or controlled variables.

Note that the above governing equations of motion are represented in terms of the true anomaly. The clustered tethered satellite system, which will be explained in the following subsection, consists of multiple tethered satellite systems located on a record disk orbit, and each of the tethered satellite system has a different longitude of the ascending node and true anomaly. This implies that the above governing equations cannot be directly integrated using the same true anomaly for the clustered tethered satellite system. Therefore, to obtain the librational motion of the clustered tethered satellite system, the above governing equations of motion must be integrated with respect to the real time and the true anomaly of each tethered satellite system by taking Eqs. (9–11) into consideration. In addition, tethered systems in elliptic orbits have a chaotic nature and thus a sophisticated control method is required to obtain and to maintain a periodic motion.

B. Record Disk Orbit

To simplify the explanation, here the center of a record disk orbit is referred to as the virtual satellite, and the other satellites, which are in formation flight with the virtual satellite, are referred to as the deputy satellites. Let the center of the virtual satellite be the origin of the reference frame to describe the position of the deputy satellites relative to the virtual satellite. Let the direction from the center of the Earth to the virtual satellite be the x-axis, and normal direction with respect to the orbital plane of the virtual satellite be the z-axis, and the cross product of the z-axis and the x-axis be the y-axis of the reference frame. This frame is referred to as the Hill's coordinate.

If no external acceleration affects the satellite, then the solutions of relative motion of the deputy satellite in the Hill's coordinate are obtained as [37]:

$$x = \frac{\dot{x}(0)}{\omega}\sin\omega t - \left(3x(0) + \frac{2\dot{y}(0)}{\omega}\right)\cos\omega t + 4x(0) + \frac{2\dot{y}(0)}{\omega} \tag{19}$$

$$y = \frac{2\dot{x}(0)}{\omega}\cos\omega t + \left(6x(0) + \frac{4\dot{y}(0)}{\omega}\right)\sin\omega t + y(0) - \frac{2\dot{x}(0)}{\omega} - (6\omega x(0) + 3\dot{y}(0))t \tag{20}$$

$$z = \frac{\dot{z}(0)}{\omega}\sin\omega t + z(0)\cos\omega t \tag{21}$$

where $(x(0), y(0), z(0))$ and $(\dot{x}(0), \dot{y}(0), \dot{z}(0))$ are the initial position and velocities, respectively.

To obtain a constant formation flight configuration, the term in Eq. (20) proportional to time t, $(6\omega x(0) + 3\dot{y}(0))$, must be set to zero, that is:

$$2\omega x(0) + \dot{y}(0) = 0 \tag{22}$$

Under this condition, the trajectory of the deputy satellite in the x-y plane is an ellipse that has its center at

$$(x_c, y_c) = \left(0, y(0) - 2\frac{\dot{x}(0)}{\omega}\right) \tag{23}$$

and minor and major radius of

$$\hat{a} = \sqrt{x^2(0) + \dot{x}^2(0)/\omega^2} \tag{24}$$

$$\hat{b} = 2\sqrt{x^2(0) + \dot{x}^2(0)/\omega^2} \tag{25}$$

in the x-axis, and y-axis, respectively. In addition, if the initial position and velocity in the z-axis are selected as

$$z(0) = x(0)\tan\psi \tag{26}$$

$$\dot{z}(0) = \dot{x}(0)\tan\psi \tag{27}$$

and ψ is selected as $\psi = \pi/3$, then the motion in the z-axis has the same phase as that in the x-axis, and the trajectory in the Hill's coordinate becomes a circle of radius

$$\sigma = 2\sqrt{x^2(0) + \dot{x}^2(0)/\omega^2} \tag{28}$$

This trajectory, shown in Fig. 4, is well known as a cart orbit, or a record disk orbit.

Figure 5 shows the geometrical relation between the inclination i and eccentricity e in the record disk orbit, which is drawn from a side view. If the relative inclination $2i$ and eccentricity e are small enough to treat the geometrical relation in term of linearity, the parameter ψ can be represented as

$$\psi = \arctan\left(\frac{i}{e}\right) \tag{29}$$

which must be $\pi/3$ to obtain a record disk orbit, therefore, the relative inclination i must be related to the eccentricity e, by

$$i = \sqrt{3}e \tag{30}$$

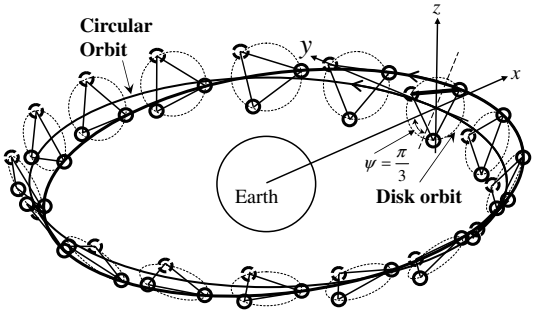

Fig. 4 Record disk orbit.

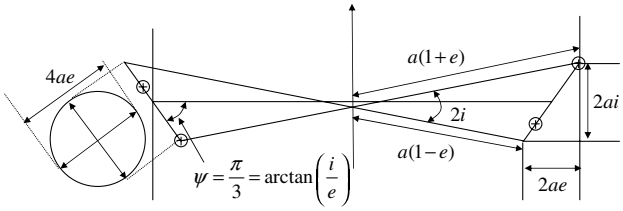

Fig. 5 Geometrical relationship of the record disk orbit.

As the result, the radius of the record disk σ is obtained as

$$\sigma = 2ae \tag{31}$$

C. Calculation of Relative True Anomaly

As mentioned earlier, because each tethered system of the clustered tethered satellite systems has different true anomaly, and changing rate of the true anomaly depends on the true anomaly, the governing equations of the tethered satellite systems cannot be directly integrated using the same true anomaly for the clustered tethered satellite systems. Therefore, to obtain the librational motion of the clustered tethered satellite systems, the equations of motion must be integrated with respect to the true anomaly of each tethered system and the real time.

In this subsection, for simplicity, we assume that the virtual satellite of the record disk is orbiting on the equator plane, the initial true anomaly is, then, determined for each tethered system on the record disk orbit. Suppose that there exist N tethered systems on the record disk orbit, and one of them, that is hereafter treated as the representative one, is located on its perigee at the initial time.

In order for the systems to form the record disk orbit under the above assumptions, the longitude of the ascending node must be distributed with the same interval of phase argument, and all the systems have the same inclination i and argument of periapsis $\varpi = \pi/2$ or $\varpi = 3\pi/2$. Because the nontilde dipole model is assumed for the Earth magnetic field, without loss of generality, the longitude of the ascending node of each system, Ω_j, can be given by

$$\Omega_j = 2\pi\frac{(j-1)}{N}, \qquad j = 1, \cdots, N \tag{32}$$

as shown in Fig. 6. The periapsis direction and orbital vectors of each system in the inertia frame, $\boldsymbol{r}_{p_j}$ and $\boldsymbol{h}_j$ are, respectively, given by

$$\boldsymbol{r}_{p_j} = \boldsymbol{C}_z(\Omega_j)\boldsymbol{C}_x(i)\boldsymbol{C}_z(\varpi)\begin{bmatrix}1\\0\\0\end{bmatrix} \tag{33}$$

$$\boldsymbol{h}_j = \boldsymbol{C}_z(\Omega_j)\boldsymbol{C}_x(i)\boldsymbol{C}_z(\varpi)\begin{bmatrix}0\\0\\1\end{bmatrix} \tag{34}$$

where $\boldsymbol{C}_x(\gamma)$ and $\boldsymbol{C}_z(\gamma)$ are direct cosine matrices that are, respectively, given by

$$\boldsymbol{C}_x(\gamma) = \begin{pmatrix}1 & 0 & 0\\ 0 & \cos\gamma & -\sin\gamma\\ 0 & \sin\gamma & \cos\gamma\end{pmatrix} \tag{35}$$

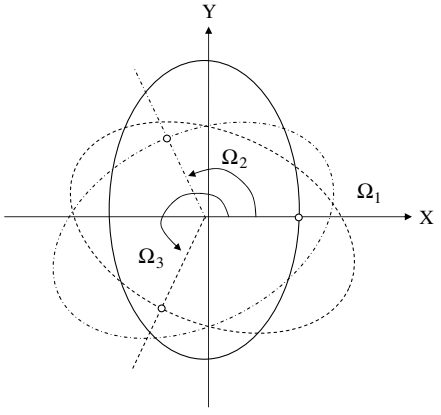

Fig. 6 Longitude of the ascending node of the system on the record disk orbit.

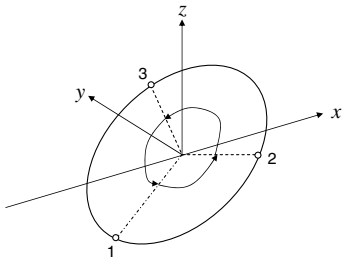

Fig. 7 Constellation flight with the same phase argument interval on a record disk orbit.

$$\boldsymbol{C}_z(\gamma) = \begin{pmatrix}\cos\gamma & -\sin\gamma & 0\\ \sin\gamma & \cos\gamma & 0\\ 0 & 0 & 1\end{pmatrix} \tag{36}$$

In addition, suppose that the tethered satellite systems are located with the same interval of phase argument on the record disk orbit, as shown in Fig. 7. In this case, recalling that the representative one is located on the perigee, and that the radius of the record disk is $\sigma = 2ae$, the position of the mass center of each tethered satellite system in the inertia frame $\boldsymbol{p}_{cm_j}$ is given by

$$\boldsymbol{p}_{cm_j} = \boldsymbol{C}_z(\Omega_1)\boldsymbol{C}_z(\varpi)\left\{\begin{pmatrix}a\\0\\0\end{pmatrix} + 2ae\begin{pmatrix}\cos(2\pi((j-1)/N)+\pi)\cos\psi\\ \sin(2\pi((j-1)/N)+\pi)\\ \cos(2\pi((j-1)/N)+\pi)\sin\psi\end{pmatrix}\right\} \tag{37}$$

As a result, the initial true anomaly of each system is determined as

$$\eta_j = \text{atan2}\left(\frac{(\boldsymbol{r}_{p_j}\times\boldsymbol{p}_{cm_j})\cdot\boldsymbol{h}_j}{|\boldsymbol{p}_{cm_j}|}, \frac{\boldsymbol{r}_{p_j}\cdot\boldsymbol{p}_{cm_j}}{|\boldsymbol{p}_{cm_j}|}\right) \tag{38}$$

It should be noted that the interval between the initial true anomalies is almost equal to $2\pi/N$, but has slight difference to form a circular record disk orbit, depending on the orbital radius and eccentricity.

III. Libration Synchronization Using Kuramoto Model

DFC is one of chaos control methods and has been widely applied to many applications. This control method is effective in stabilizing chaotic motions to a periodic motion, but needs to record the past data. Recording past data is undesired for space systems, because memory resources are limited in such systems. To overcome this problem, we propose Kuramoto model-based control methods to synchronize the librational motion of CEDTS.

The Kuramoto model is a mathematical model that can be used to describe synchronized behavior of a large set of coupled oscillators, such as chemical and biological oscillators, and many other applications. This model usually makes the following three assumptions: 1) there is weak coupling; 2) the oscillators are identical or nearly identical, and 3) interactions depend on the phase difference between each pair of objects. The most popular form of the Kuramoto model has the following governing equations:

$$\frac{\mathrm{d}\xi_i}{\mathrm{d}t} = \nu_i + \frac{K}{N}\sum_{j=1, j\neq i}^{N}\sin(\xi_j - \xi_i), \qquad i = 1, \cdots, N \tag{39}$$

In this model, the phase difference is used to give the feedback to the systems. If the force among the systems is attractive, the phase difference among the systems becomes zero gradually, that is, the

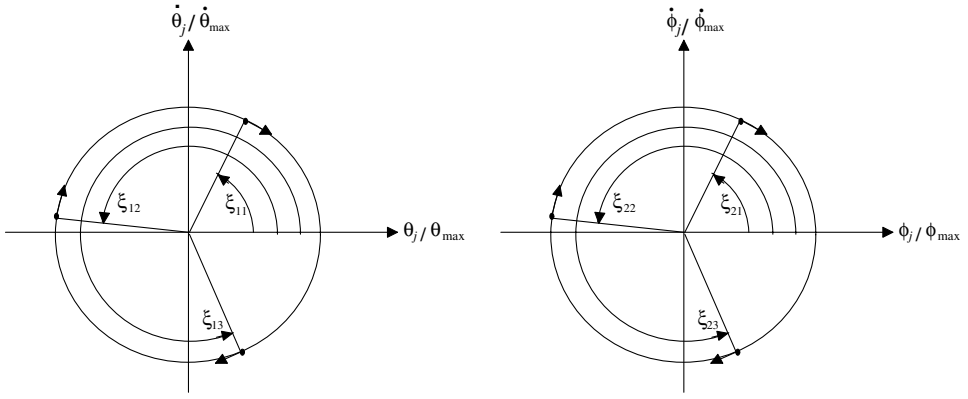

a) Controller-1 **b) Controller-2**

Fig. 8 Definition of phase arguments ξ for the Kuramoto model-based control methods.

oscillation of all the systems is gradually synchronized. On the other hand, the force among the systems is repulsive, the phase difference among the systems becomes the same, that is, the oscillation of all the systems gradually converges to the one with a bias phase difference between each other.

To apply the Kuramoto model to the librational control of the CEDTS, we need to consider which component of the CEDTS corresponds to the phase argument ξ_i in the Kuramoto model. In addition, to design good controllers, we should take into consideration that DFC for librational motion of TSS presented in the past papers showed good ability to stabilize chaotic motions to a periodic motion.

The DFC methods applied to the in-plane librational control of EDT are often expressed as

$$I = K_{dfc}(\dot{\theta}(t) - \dot{\theta}(t-\tau))$$

It should be noted that librational angular velocity was used as the control signal to determine the control input of the DFC in past studies, while the control signal in the Kuramoto model is the difference between the phase arguments of system's motion.

Although there is a difference between the above two control methods, if the angular velocity difference in a delayed feedback control is interpreted as a kind of phase difference corresponding to that of the Kuramoto model, the above two controllers become very similar. It is natural that the chaos controllers have similarity because their objective is basically the same, that is, to stabilize chaotic motions to a periodic motion.

To consider the periodic librational motion as a simple oscillation, the phase arguments ξ_{1j} and ξ_{2j}, which will be used in the Kuramoto model-based controller, are defined using θ_{max}, $\dot{\theta}_{max}$, ϕ_{max}, $\dot{\phi}_{max}$, θ_j, ϕ_j, $\dot{\theta}_j$, and $\dot{\phi}_j$, as

$$\xi_{1j} := \text{atan2}(\dot{\theta}_j/\dot{\theta}_{max}, \theta_j/\theta_{max}) \tag{40}$$

$$\xi_{2j} := \text{atan2}(\dot{\phi}_j/\dot{\phi}_{max}, \phi_j/\phi_{max}) \tag{41}$$

as shown in Figs. 8a and 8b.

In this paper, we consider a triangle formation flight of EDT systems, that is, the number of the EDT systems N is set to three. By taking into account that the librational motion of each tethered system has a bias phase argument of $2\pi/N$, the following two Kuramoto model-based control methods are considered to determine the time-varying electrodynamic parameter ε_i for each electrodynamic tether which is intended to keep the phase difference of in-plane/out-of-plane librational motion between each electrodynamic tethered system to $2\pi/3$.

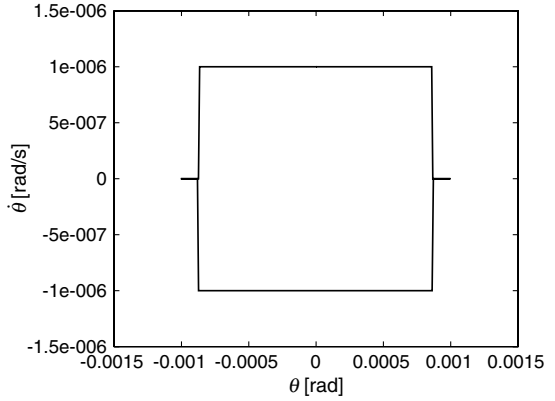

a)

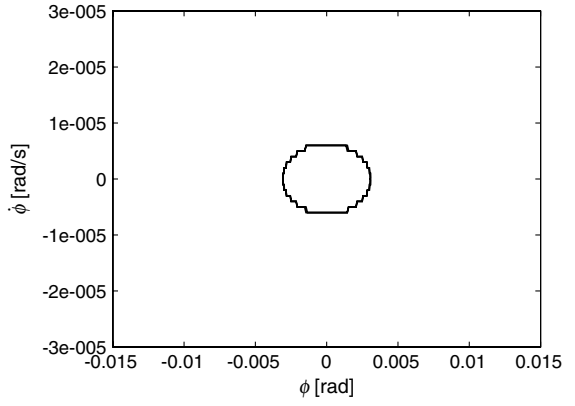

b)

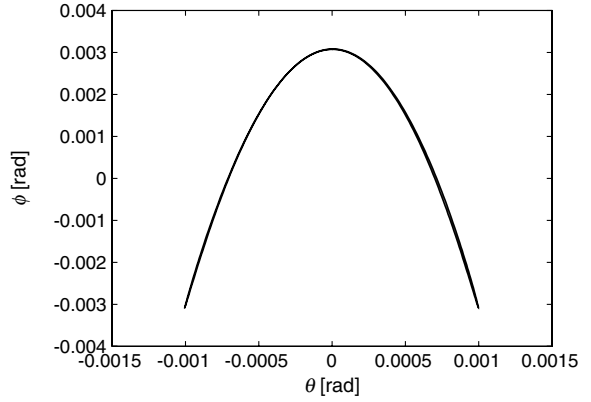

c)

Fig. 9 Trajectories of the 2π-periodic motion in the θ-$\dot{\theta}$ plane (a), ϕ-$\dot{\phi}$ plane (b), and θ-ϕ plane (c) for the case of $e = 0.001$.

Kuramoto Model-Based Control-1

$$\begin{aligned}\varepsilon_1 &= K\{\mathbf{sin}((\xi_{12}-\alpha)-\xi_{11})+\mathbf{sin}((\xi_{13}+\alpha)-\xi_{11})\}\\ \varepsilon_2 &= K\{\mathbf{sin}((\xi_{11}+\alpha)-\xi_{12})+\mathbf{sin}((\xi_{13}-\alpha)-\xi_{12})\}\\ \varepsilon_3 &= K\{\mathbf{sin}((\xi_{11}-\alpha)-\xi_{13})+\mathbf{sin}((\xi_{12}+\alpha)-\xi_{13})\}\end{aligned} \tag{42}$$

Kuramoto Model-Based Control-2

$$\begin{aligned}\varepsilon_1 &= K\{\mathbf{sin}((\xi_{22}-\alpha)-\xi_{21})+\mathbf{sin}((\xi_{23}+\alpha)-\xi_{21})\}\\ \varepsilon_2 &= K\{\mathbf{sin}((\xi_{21}+\alpha)-\xi_{22})+\mathbf{sin}((\xi_{23}-\alpha)-\xi_{22})\}\\ \varepsilon_3 &= K\{\mathbf{sin}((\xi_{21}-\alpha)-\xi_{23})+\mathbf{sin}((\xi_{22}+\alpha)-\xi_{23})\}\end{aligned} \tag{43}$$

where α is the bias phase argument, which should be set to $2\pi/3$ for the case of the triangle formation flight.

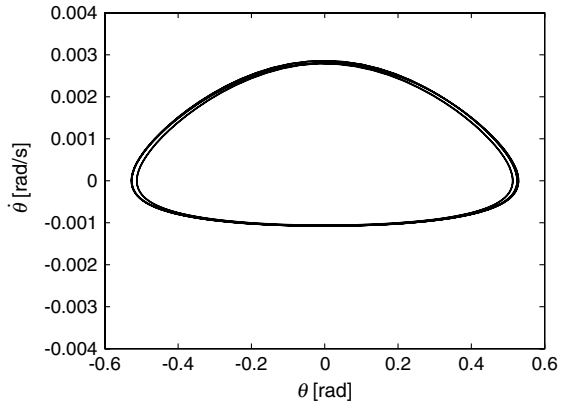

a)

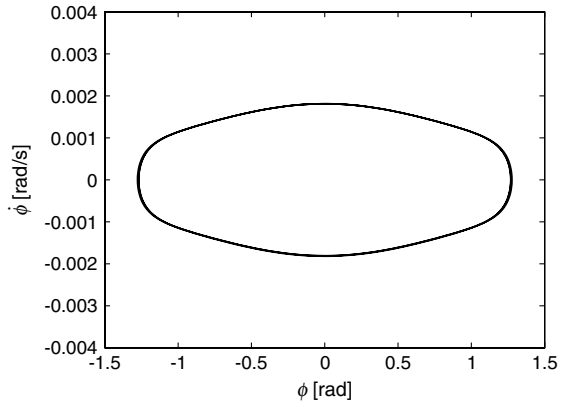

b)

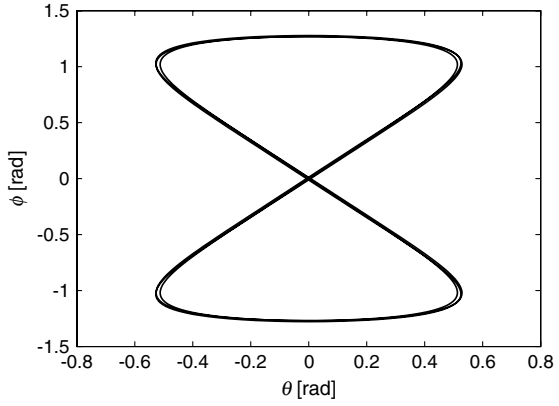

c)

Fig. 10 Trajectories of the 4π-periodic motion in the θ-$\dot{\theta}$ plane (a), ϕ-$\dot{\phi}$ plane (b), and θ-ϕ plane (c) for the case of $e = 0.001$.

Table 1 Simulation parameters for the orbital elements

	EDT-1	EDT-2	EDT-3
ϖ, rad	$3\pi/2$	$3\pi/2$	$3\pi/2$
Ω_j, rad	0	$2\pi/3$	$4\pi/3$
Initial η_j, rad	0	-2.096127	2.096127

Note that the magnitude of the control input determined by the Kuramoto model-based control is always limited within $2K$, because it is given by $K(\sin(\,) \pm \sin(\,))$.

IV. Numerical Simulations

A. Periodic Solutions

To demonstrate the effectiveness and validity of the proposed control schemes, numerical simulations are carried out. Orbital radius and eccentricity are chosen as $a = 7500$ km, and $e = 0.001$, respectively. In this case, the radius of the record disk is determined as $\sigma = 2ae = 15$ km. The inclination for the record disk orbit must be $i = \sqrt{3}e$, thus, the inclination is set to $i = 0.001732$ rad.

First, we obtain the periodic motion of one tethered system for the above case without any electrodynamic interation, $\varepsilon = 0$, that is, periodic solutions for the gravity gradient tethered system, using Newtown–Raphson method. Figures 9a–9c show the trajectories of the obtained periodic motion in the θ-$\dot{\theta}$ plane, ϕ-$\dot{\phi}$ plane, and the θ-ϕ plane, respectively. It is shown in the figures that the magnitude of the trajectories is small, and that the trajectory in the in-plane phase plane looks rectangular. In addition, the trajectory in the θ-ϕ plane is asymmetric with respect to the origin, and looks like mathematical symbol $\wedge$. This periodic motion corresponds to a 2π-periodic

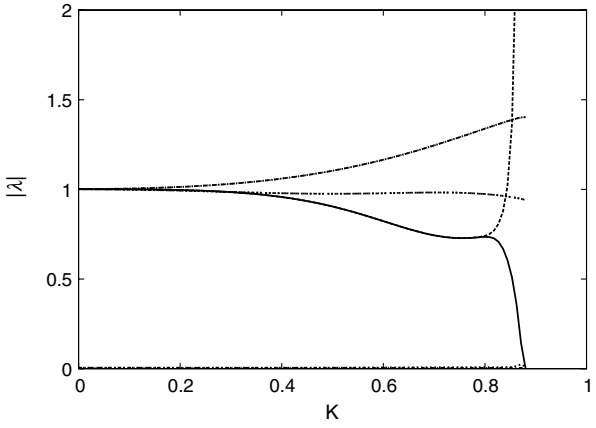

a) Kuramoto-model based control-1

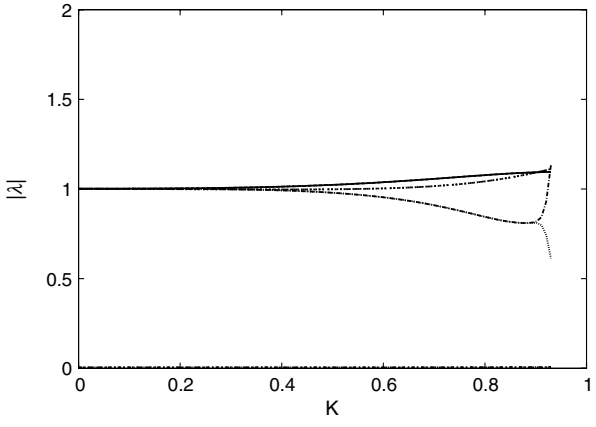

b) Kuramoto-model based control-2

Fig. 11 Moduli vs control gain for the 4π-periodic solution.

Table 2 Simulation parameters for the tether angles

	EDT-1	EDT-2	EDT-3
Initial θ_i, rad	0.152856	0.144627	0.145055
Initial ϕ_i, rad	0.242423	0.205312	0.283360
Initial $\dot{\theta}_i$, rad/s	−0.001036	−0.001047	−0.001049
Initial $\dot{\phi}_i$, rad/s	−0.001770	−0.001755	−0.001762

solution given in [23–25], and is likely to change to another motion whose shape in the in-plane and out-of-planes is upside down. Therefore, it may be difficult to apply the Kuramoto model-based control methods to this periodic solution, because the Kuramoto model assumes systems, each of which has a simple oscillation that could be represented as a circular trajectory in the phase plane. This feature is the limitation of the control methods based on the Kuramoto model when they are intended to be applied to stabilize certain periodic librational motions that do not correspond to simple oscillations.

Figures 10a–10c show the trajectories of another periodic motion, in the θ-$\dot{\theta}$ plane, ϕ-$\dot{\phi}$ plane, and θ-ϕ plane, respectively. The magnitude of trajectories is much greater than that of the previous periodic motion. The trajectory in θ-ϕ is symmetric with respect to the origin, and looks like number eight. This periodic solution is the same as those presented in the past studies [23–25]. In this periodic solution, the in-plane tether angle oscillates twice during period when the out-of-plane tether angle oscillates one. This periodic motion corresponds to a 4π-periodic solution, because tether angles return to the origin in this periodic motion when the center of mass of the system completes orbital motion of two orbits. During true anomaly change of 4π, the in-plane tether angle oscillates 6 times, and the out-of-plane tether angle oscillates 3 times. Contrary to the above 2π-periodic solution, this 4π-periodic motion could be easily maintained by a Kuramoto model-based control, because the trajectories of this periodic motion are symmetric, and their motions are simple oscillations. This expectation will be verified by numerical simulations. Because the tethered system almost points to the vertical line, and does not widely librate in the 2π-periodic solution, hereinafter, we only focus on the 4π-periodic solution.

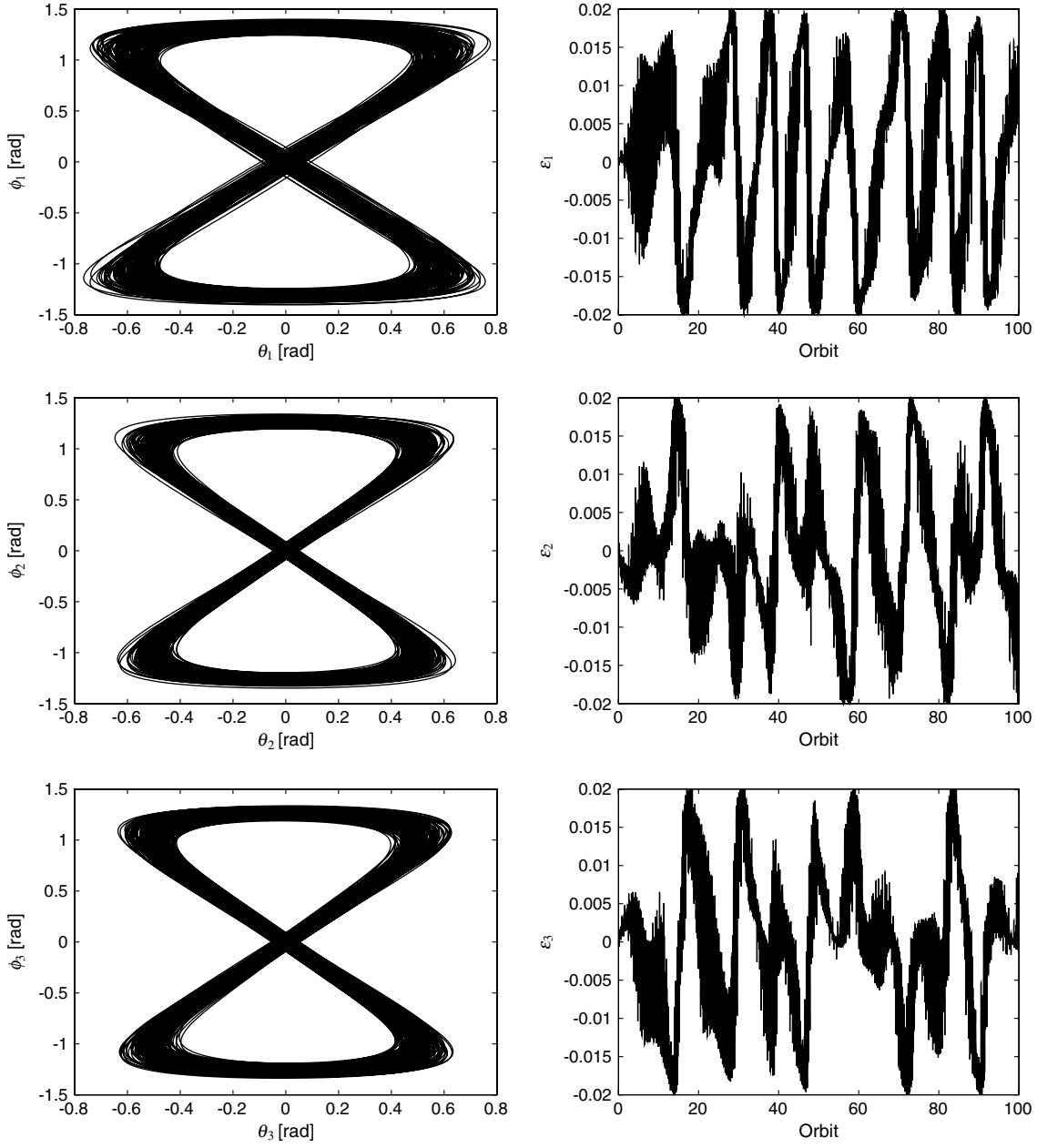

Fig. 12 Trajectories of the tether angles and time responses of electrodynamic parameters for case-1: the Kuramoto model-based control-1 with control gain $K = 0.01$.

B. Stability Analysis of the Kuramoto Model-Based Control Methods

Referring to the obtained periodic trajectories, the parameters $\theta_{\max}$, $\dot{\theta}_{\max}$, $\phi_{\max_j}$ and $\dot{\phi}_{\max_j}$ for the 4π-periodic solution are determined as $\theta_{\max} = 0.528608$ rad, $\dot{\theta}_{\max} = 0.002858$ rad/s, $\phi_{\max} = 1.277341$ rad, and $\dot{\phi}_{\max} = 0.001813$ rad/s. The argument of perigee and longitude of the ascending node are set as listed in Table 1, then the initial true anomaly is determined for each tethered system.

To appropriately choose the control gain for the Kuramoto model-based control, here we analyze the stability of the control methods in accordance with Floquet's theorem. Monodromy matrix is a matrix to express how much the state variables that are slightly perturbed from a periodic motion diverge from or converge to the periodic motion after one period of the periodic motion, and the modulus is the absolute value of a complex eigenvalue of the monodromy matrix. If all the moduli of eigenvalues of the monodromy matrix are less than or equal to one, then the periodic solution will not diverge, while there is at least one muduli greater than one, then the system will diverge as time increases.

The monodromy matrix for the closed-loop system of the Kuramoto model-based control methods is obtained as $\boldsymbol{M}(\tau)$ by integrating the following couple of equations over a period of $t \in [0, \tau]$

$$\dot{\boldsymbol{x}} = \boldsymbol{f}(\boldsymbol{x}(t), \boldsymbol{\varepsilon}(\boldsymbol{x})) \tag{44}$$

$$\dot{\boldsymbol{M}} = \left(\frac{\partial \bar{\boldsymbol{f}}}{\partial \bar{\boldsymbol{x}}}\right)\boldsymbol{M} \tag{45}$$

with the initial conditions $\boldsymbol{x}(0)$, that is, the initial values in the periodic solution, and $\boldsymbol{M}(0) = \boldsymbol{I}_{12\times 12}$, that is, an eigenmatrix with dimension of 12×12. If all the moduli of the monodromy matrix $\boldsymbol{M}(\tau)$ are smaller than, or equal to unity, then the Kuramoto model-based control method will be able to keep the periodic solutions.

Figure 11 shows the moduli of eigenvalues of the monodromy matrix for the closed loop of the Kuramoto model-based control methods. Although the dimension of the monodromy matrix is 12, the number of individual moduli is 4 or 5. This is because the three

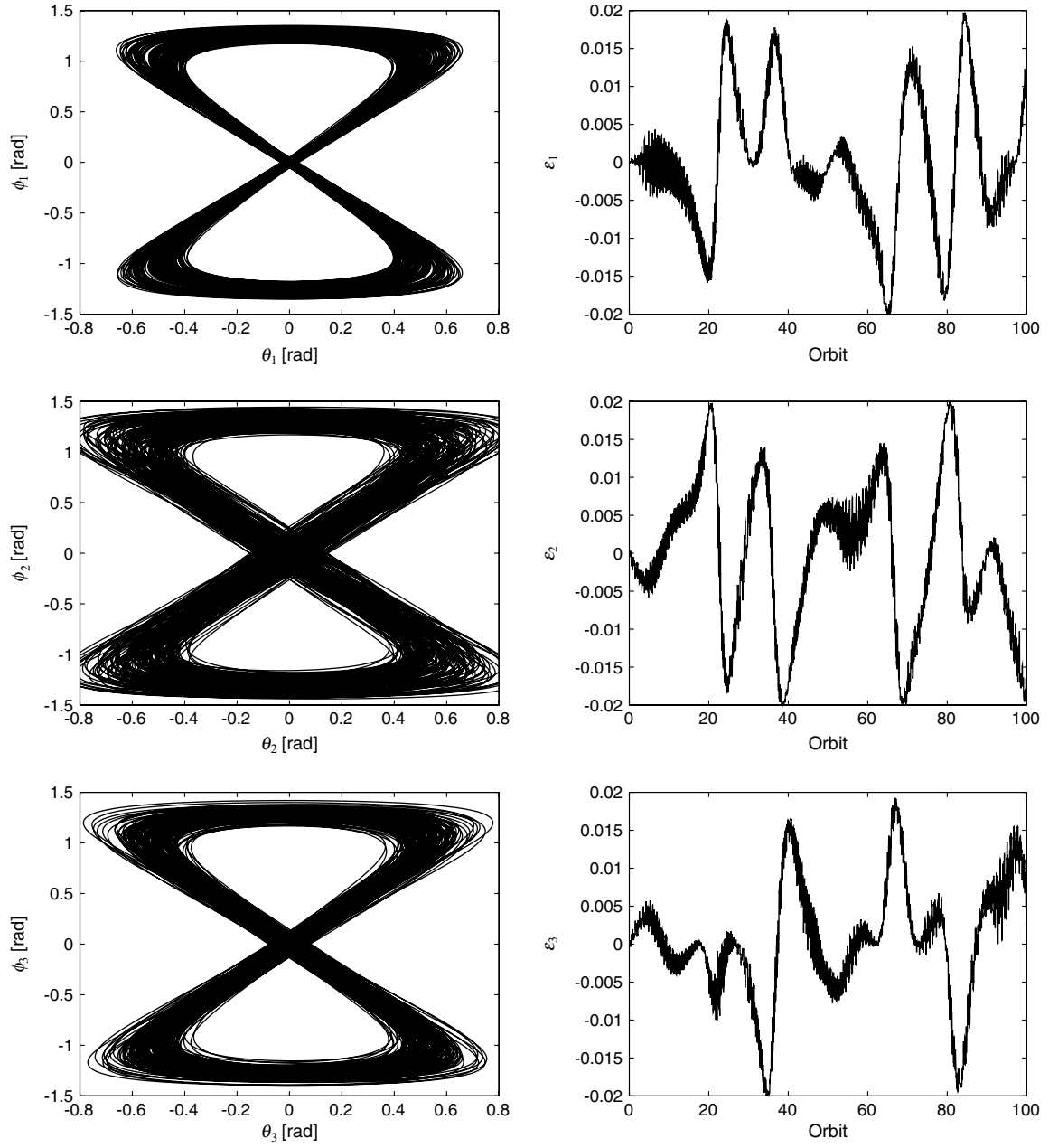

Fig. 13 Trajectories of the tether angles and time responses of electrodynamic parameters for case-2: the Kuramoto model-based control-2 with control gain $K = 0.01$.

tethered systems in the CEDTS are identical, then moduli appear in form of degeneracy. When the number of moduli is 5, the moduli contains an effect of the true anomaly variation, because in this study the equations of motion for the total systems are calculated by treating time as the independent variable, but not the true anomaly.

For the Kuramoto model-based controller-1, one of the moduli becomes greater than unity when the control gain K is greater than about 0.1. In addition, it is found that when the control gain $K = 0.8$, a bifurcation occurs where one modulus less than unity splits into two, one of them becomes greater than unity, and the other one keeps less than unity. Similarly, two of the moduli for the Kuramoto model-based controller-2 are greater than unity when the control gain K is greater than about 0.4, while the excess rate for the Kuramoto model-based controller-2 is smaller than that of the controller-1. When the control gain is $K = 0.9$, a bifurcation of moduli occurs for the controller-2. The reason why the excess rate for the controller-2 is slower than that of the controller-1 can be explained as follows. For the case of the controller-2, the electrodynamic parameters are determined from the out-of-plane tether motion, while the Lorentz force has an effect towards in-plane direction. On the other hand, for the case of the controller-1, the electrodynamic parameters are determined from the in-plane motion that has the same direction as that of the Lorentz force effect.

By taking into the stability analysis into consideration, to study the effect of the control gain on the periodic librational motion of the clustered electrodynamic tethered system, we have selected two control gains for the following numerical simulations; $K = 0.01$, and $K = 0.4$. When the control gain $K = 0.01$, the maximum modulus is $|\lambda| = 1.0008$ for the controller-1, and $|\lambda| = 1.001$ for the controller-2. On the other hand, when the control gain is $K = 0.4$, the maximum modulus is $|\lambda| = 1.059$ for the controller-1, while $|\lambda| = 1.012$ for the controller-2. The moduli are slightly greater than the unity for the control gain $K = 0.01$, but the excess is very small. As the results of stability analysis, we predict that the librational motion can be kept around the 4π-periodic motion for the case of $K = 0.01$, whereas they will gradually diverge from the periodic motion for the case of $K = 0.4$. This prediction will be verified by the following numerical simulations.

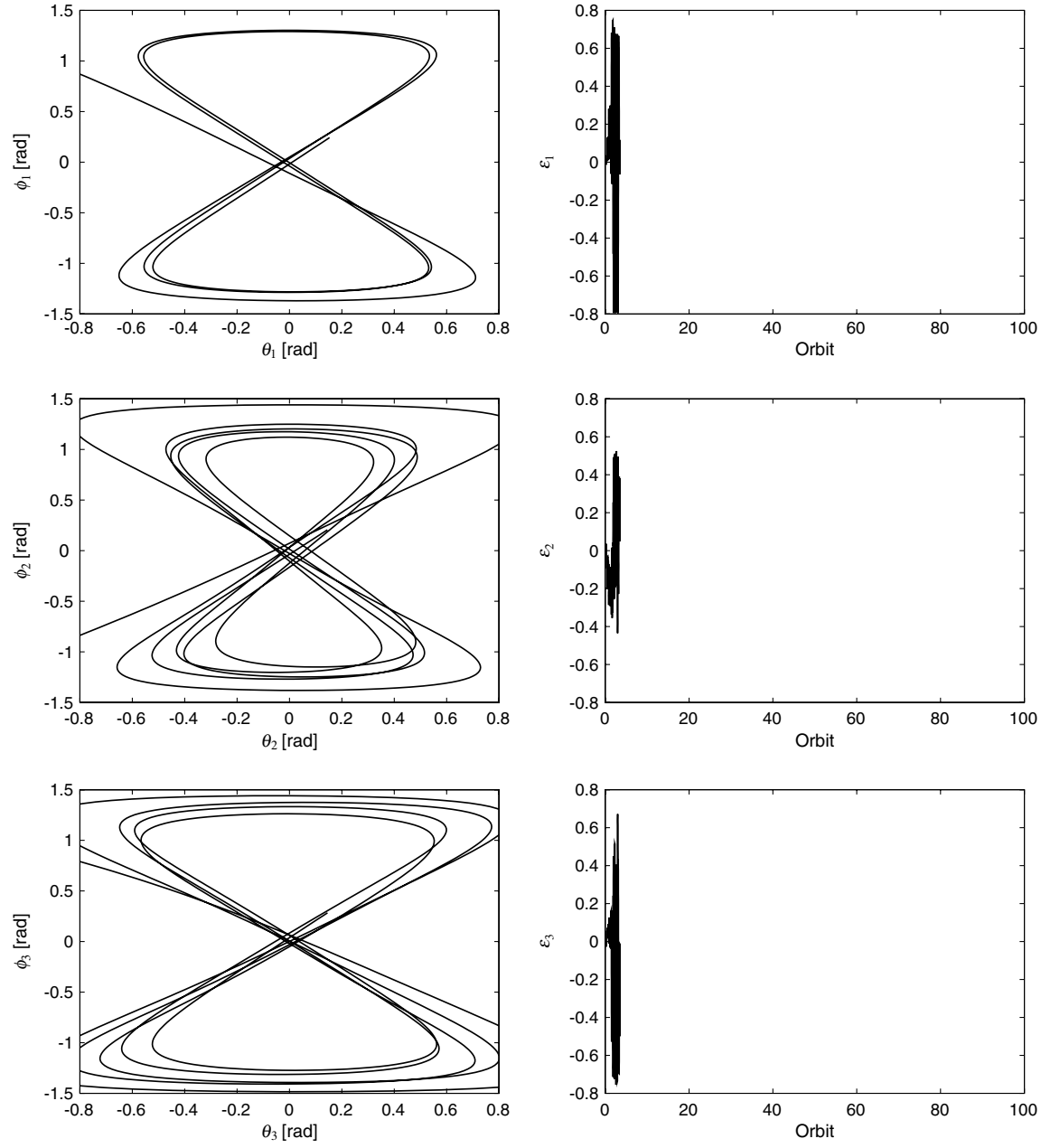

Fig. 14 Trajectories of the tether angles and time responses of electrodynamic parameters for case-3: the Kuramoto model-based control-1 with control gain $K = 0.4$.

C. Numerical Results of the Kuramoto Model-Based Control Methods

Taking into account the bias phase argument $\alpha = 2\pi/3$, the initial angles and angular velocities are selected, as listed in Table 2 for the 4π-periodic motion. Note that to give slight perturbation at the initial time, the initial tether angles of EDT-2 and EDT-3 are set not to be symmetric with each other.

As the results of the combination of control methods, and control gains, we have considered the following four cases:

1) Case-1: Kuramoto model-based control-1 with control gain $K = 0.01$

2) Case-2: Kuramoto model-based control-2 with control gain $K = 0.01$

3) Case-3: Kuramoto model-based control-1 with control gain $K = 0.4$

4) Case-4: Kuramoto model-based control-2 with control gain $K = 0.4$

We have calculated the tether motions for 100 orbits or until the state variables diverged, using the fourth order adaptive stepsize controlled Runge–Kutta scheme, or ode45 provided by MATLAB™. The results of numerical simulations corresponding to the above four cases are shown in Figs. 12–15. In those figures, trajectories in the (θ, ϕ) plane and time responses of the electrodynamic parameter ε are shown for each tethered system.

We can see in Fig. 12 that the 4π-periodic motion was maintained by the Kuramoto model-based control-1 with control gain $K = 0.01$. The electrodynamic parameter resulting from the Kuramoto model-based control-1 changed with combination of one orbit and harmonic periods of 4π-periodic motion (2 orbits), i.e, 10 orbits. As mentioned above, this is because the librational motion of the tethered systems in elliptic orbits is chaotic, thus not only the period of periodic motion (2 orbits), but also harmonic periods of the periodic motion could be contained in the system. It is not easy to predict this long period of about 10 orbits in the oscillation of electrodynamic parameters ε from the results of linear stability analysis.

The results for case-2 are shown in Fig. 13. Similar to the results for case-1, the 4π-periodic motion was successfully kept by the Kuramoto model-based control-2 with control gain $K = 0.01$.

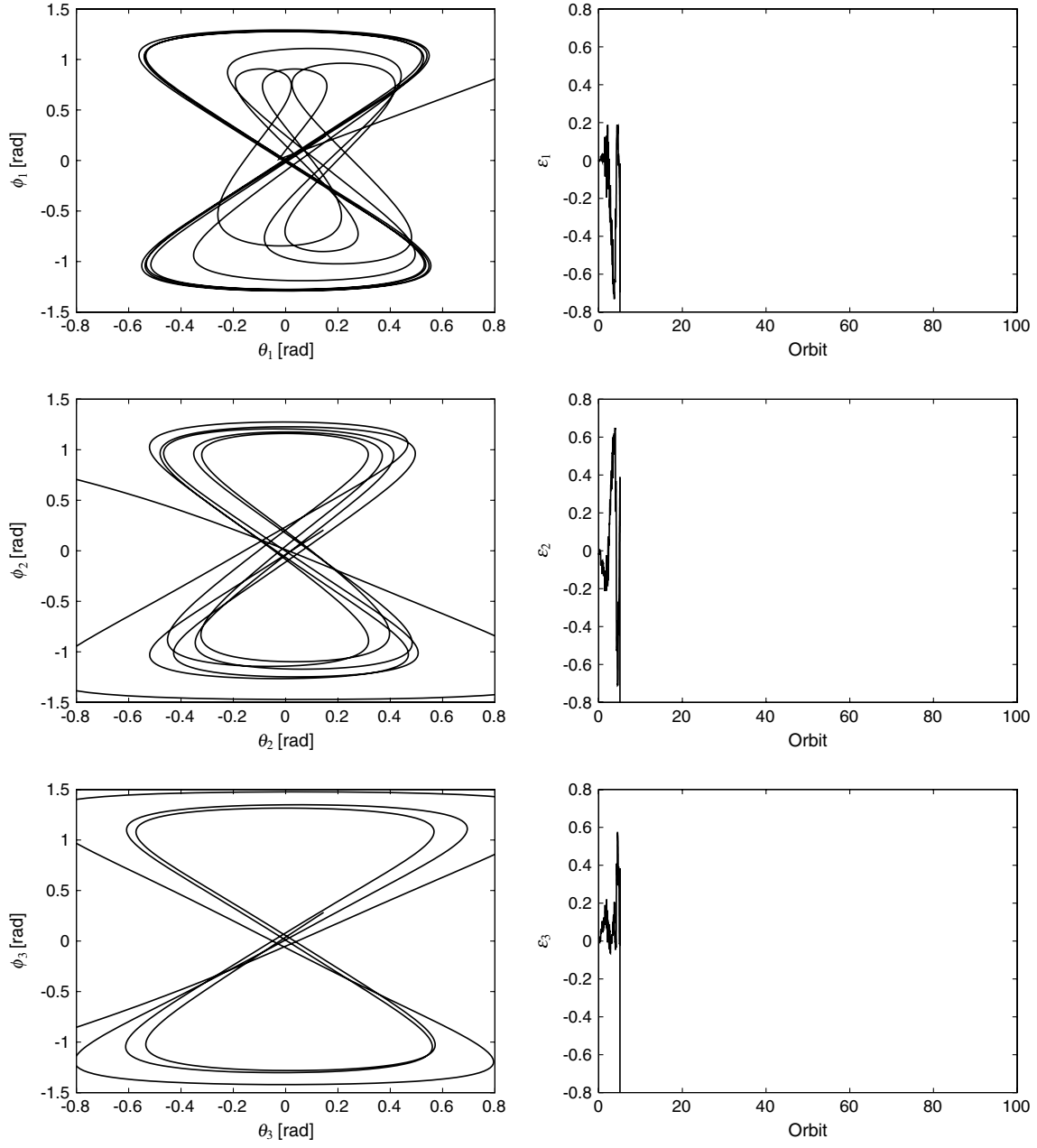

Fig. 15 Trajectories of the tether angles and time responses of electrodynamic parameters for case-4: the Kuramoto model-based control-2 with control gain $K = 0.4$.

However, contrary to the results for case-1, the magnitude of the librational motions of electrodynamic tethered systems 2 and 3 gradually becomes greater than that for case-1. This is because as mentioned above the maximum modulus for the controller-2 with the control gain $K = 0.01$ is slightly greater than that of the controller-1 with the same control gain. In addition, the electrodynamic parameters oscillate with combination of a period of one orbit and about a period of 18 orbits. This longer period of 18 orbits is different from that for case-1, but both the periods are harmonic period of the periodic motion. This long period for the controller-2 with $K = 0.01$ was not predicted before the numerical simulations, and it may depend on the control gain and nonlinear characteristics of the system. We will have to analyze the dependency of this long period on the control gain and other parameters in near future.

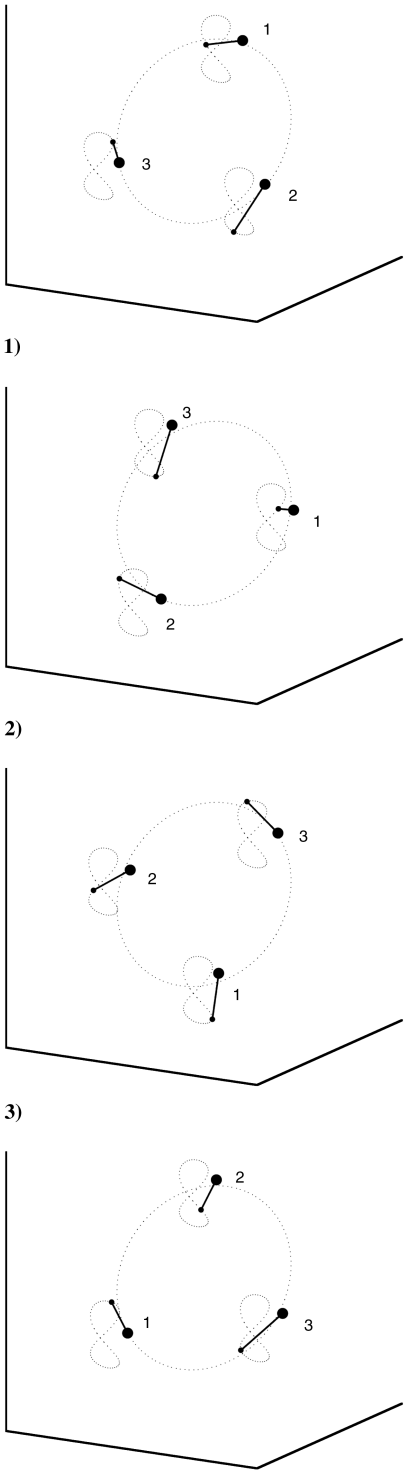

Fig. 16 Animation of the librational motion of the clustered electrodynamic tether system, along with the trajectories of the record disk and the 4π periodic motion.

Furthermore, it is interesting to see that the time responses of two electrodynamic parameters seem to be in antiphase with each other during some duration, i.e., ε_1 and ε_2 between 60 and 80 orbits for case-1. This may imply that phase arguments of the electrodynamic tethered systems 1 and 2 during the above duration are vibrating against that of the EDT-3. A similar phenomena was observed in the time responses of ε_1 and ε_2 between 70 and 100 orbits for case-2. This motion can be regarded as one of vibration modes, and another mode could appear, depending on simulation parameters and initial conditions.

Contrary to cases-1 and 2, the 4π-periodic motions diverged soon after a few orbits for cases-3 and 4, as shown in Figs. 14 and 15. This is because one of the moduli is greater than unity for the Kuramoto model-based control methods with control gain $K = 0.4$, as shown in Figs. 11a and 11b. In accordance with Floquet's theorem, the periodic motion cannot be maintained by any controller if one modulus greater than unity exists in the system.

As the final figure, the 4π-periodic librational motion of the clustered electrodynamic tethered satellite systems is shown in Fig. 16, along with the trajectory of the periodic motion and the record disk orbit. As shown in Fig. 16, the center of mass of the tethered system is located on the record disk orbit with the same phase argument interval, tether angles of each system are not the same at the initial time, and their interval is about $2\pi/3$ in the phase plane.

These results show that the Kuramoto model-based control methods are capable of synchronizing librations of the clustered electrodynamic tethered systems that behave with a 4π-periodic solution for the case that electrodynamic parameters are determined by the phase argument of the periodic motions and the control gain is chosen appropriately from the results of stability analyses based on Floquet's theorem.

V. Conclusions

In this paper, a new configuration of electrodynamic tether system called CEDTS has been proposed, which keeps multiple electrodynamic tethered systems constrained to a "record disk" orbit. This configuration can be regarded as a formation flight configuration both toward in-plane and out-of-plane direction, because it inherits advantages from the formation flight satellites set on a record disk orbit, and tethered systems.

To synchronize the librational motion of CEDTS, the Kuramoto model has been applied to determine the electric current on the tethers. In this study, two kinds of Kuramoto model-based control methods were considered. The control input for the first control method is determined from the phase argument of the in-plane motion, and for the second one from that of the out-of-plane motion. The Kuramoto model-based control methods were applied to a 4π-periodic motion.

The results of numerical simulations have shown that the 4π-periodic motion was successfully synchronized among the electrodynamic tether systems by the proposed Kuramoto model-based control methods with the appropriately chosen control gain.

The dumbbell model used in this study to represent each electrodynamic tether system is, however, simple, and the center of the record disk is assumed to orbit on the equator plane. These assumptions are not always necessary. Only two cases were studied for the control gain in this study. Thus, a more realistic model, which includes tether flexibility, inclination for a record disk orbit, and so on, and dependency of the oscillations among the electrodynamic parameters on the control gain, will have to be studied in the future.

Acknowledgment

This study was supported in part by a grant from Kurata Memorial Hitachi Science and Technology.

References

[1] Stebbins, R., "LISA Mission Tutorial," *AIP Conference Proceedings*, Vol. 873, American Inst. of Physics, Melville, NY, 2006, pp. 3–12. doi:10.1063/1.2405016

[2] Scharf, D. P., Hadaegh, F. Y., and Ploen, S. R., "A Survey of Spacecraft Formation Flying Guidance and Control (Part I): Guidance," *Proceedings of the American Control Conference*,Vol. 2, IEEE Publications, Piscataway, NJ, 2003, pp. 1733–1739.

[3] Scharf, D. P., Hadaegh, F. Y., and Ploen, S. R., "A Survey of Spacecraft Formation Flying Guidance and Control (Part II): Control," *Proceedings of the American Control Conference*, Vol. 4, IEEE Publications, Piscataway, NJ, 2004, pp. 2976–2985.

[4] Cosmo, M. L., and Lorenzini, E. C., *Tethers in Space Handbook*, 3rd ed., Cambridge, NASA Marshall Space Flight Center and Smithsonian Astrophysical Observatory, 1977.

[5] Schechter, H. B., "Dumbbell Librations in Elliptic Orbits," *AIAA Journal*, Vol. 2, No. 6, 1964, pp. 1000–1003. doi:10.2514/3.2489

[6] Modi, V. J., and Brereton, R. C., "Periodic Solutions Associate with the Gravity-Gradient-Oriented System: Part I. Analytical and Numerical Determination," *AIAA Journal*, Vol. 7, No. 7, 1969, pp. 1217–1225. doi:10.2514/3.5325

[7] Brereton, R. C., and Modi, V. J., "Periodic Solutions Associate with the Gravity-Gradient-Oriented System: Part II. Stability Analysis," *AIAA Journal*, Vol. 7, No. 8, 1969, pp. 1465–1468. doi:10.2514/3.5416

[8] Brereton, R. C., and Modi, V. J., "Stability of the Planar Librational Motion of a Satellite in an Elliptic Orbit," *Proceedings of the XVII International Astronautical Congress*, Vol. 4, Gordon and Breach, New York, 1967, pp. 179–192.

[9] Swan, P. A., "Dynamics and Control of Tethers in Elliptical Orbits," Ph.D., Dissertation, Univ. of California, Los Angeles, 1984.

[10] Kumar, K., and Kumar, K. D., "Open-loop Satellite Librational Control in Elliptic Orbits through Tether," *Acta Astronautica*, Vol. 41, No. 1, 1997, pp. 15–21. doi:10.1016/S0094-5765(97)00217-8

[11] Fujii, H. A., and Ichiki, W., "Nonlinear Dynamics of the Tethered Subsatellite in the Station Keeping," *Journal of Guidance, Control, and Dynamics*, Vol. 20, No. 2, 1997, pp. 403–406. doi:10.2514/2.4057

[12] Fujii, H. A., Ichiki, W., Suda, S., and Watanabe, T. R., "Chaos Analysis on Librational Control of Gravity-Gradient Satellite in Elliptic Orbit," *Journal of Guidance, Control, and Dynamics*, Vol. 23, No. 1, 2000, pp. 146–146. doi:10.2514/2.4500

[13] Pyragas, K., "Continuous Control of Chaos by Self-Controlling Feedback," *Physics Letters A*, Vol. 170, No. 6, 1992, pp. 421–428. doi:10.1016/0375-9601(92)90745-8

[14] Takeichi, N., Natori, M. C., and Okuizumi, N., "Dynamic Behavior of a Tethered System with Multiple Subsatellites in Elliptic Orbits," *Journal of Spacecraft and Rockets*, Vol. 38, No. 6, 2001, pp. 914–921. doi:10.2514/2.3763

[15] Takeichi, N., Natori, M. C., and Okuizumi, N., "Fundamental Strategies for Control of a Tethered System in Elliptical Orbits," *Journal of Spacecraft and Rockets*, Vol. 40, No. 1, 2003, pp. 119–125. doi:10.2514/2.3924

[16] Takeichi, N., Natori, M. C., and Okuizumi, N., "In-Plane/Out-of-Plane Librations of a Tethered System in Elliptical Orbits," *Transactions of the Japan Society for Aeronautical and Space Sciences*, Vol. 43, No. 142, 2001, pp. 196–202. doi:10.2322/tjsass.43.196

[17] Kojima, H., Iwasaki, M., Fujii, H. A., Blanksby, C., and Trivailo, P., "Nonlinear Control of Librational Motion of Tethered Satellites in Elliptic Orbits," *Journal of Guidance, Control, and Dynamics*, Vol. 27, No. 2, 2004, pp. 229–239. doi:10.2514/1.9166

[18] Kojima, H., and Sugimoto, T., "Nonlinear Control of a Double Pendulum Electrodynamic Tether System," *Journal of Spacecraft and Rockets*, Vol. 44, No. 1, 2007, pp. 280–284. doi:10.2514/1.24537

[19] Kojima, H., and Sugimoto, T., "Stability analysis of In-plane and Out-of-plane Periodic Motions of Electrodynamic Tether System in Inclined Elliptic Orbit," *Acta Astronautica*, Vol. 65, Nos. 3–4, 2009, pp. 477–488. doi:10.1016/j.actaastro.2009.02.006

[20] Ushio, T., "Limitation of Delayed Feedback Control in Non-linear Discrete-Time Systems," *IEEE Transactions on Circuits and Systems, Part I*, Vol. 43, No. 9, 1996, pp. 815–816. doi:10.1109/81.536757

[21] Kojima, H., and Sugimoto, T., "Switching Delayed Feedback Control of Electrodynamic Tether System in Elliptic Orbit," *Acta Astronautica*, Vol. 66, Nos. 7–8, 2010, pp. 1072–1080. doi:10.1016/j.actaastro.2009.09.014

[22] Peláez, J., Ruiz, M., and Lopez-Rebollat, S., "Two-Bar Model for the Dynamics and Stability of Electrodynamic Tethers," *Journal of Guidance, Control, and Dynamics*, Vol. 25, No. 6, 2002, pp. 1125–1135. doi:10.2514/2.4992

[23] Peláez, J., and Lara, M., "Periodic Solutions in Electrodynamic Tethers on Inclined Orbits," *Journal of Guidance, Control, and Dynamics*, Vol. 26, No. 3, 2003, pp. 395–406. doi:10.2514/2.5077

[24] Peláez, J., and Lorenzini, E. C., "Libration Control of Electrodynamic Tethers in Inclined Orbit," *Journal of Guidance, Control, and Dynamics*, Vol. 28, No. 2, 2005, pp. 269–279. doi:10.2514/1.6473

[25] Peláez, J., and Andres, Y. N., "Dynamics Stability of Electrodynamic Tethers in Inclined Elliptical Orbits," *Journal of Guidance, Control, and Dynamics*, Vol. 28, No. 4, 2005, pp. 611–622. doi:10.2514/1.6685

[26] Williams, P., "Libration Control of Tethered Satellites in Elliptical Orbits," *Journal of Spacecraft and Rockets*, Vol. 43, No. 2, 2006, pp. 476–479. doi:10.2514/1.17499

[27] Williams, P., Watanabe, T., Blanksby, C., Trivailo, P., and Fujii, H. A., "Libration Control of Flexible Tethers Using Electromagnetic Forces and Movable Attachment," *Journal of Guidance, Control, and Dynamics*, Vol. 27, No. 5, 2004, pp. 882–897. doi:10.2514/1.1895

[28] Williams, P., "Electrodynamic Tethers Using Forces-Current Variations Part I: Periodic Solutions for Tether Librations," *Journal of Spacecraft and Rockets*, Vol. 47, No. 2, 2010, pp. 308–319. doi:10.2514/1.45731

[29] Williams, P., "Electrodynamic Tethers Under Forced-Current Variations Part II: Flexible-Tether Estimation and Control," *Journal of Spacecraft and Rockets*, Vol. 47, No. 2, 2010, pp. 320–333. doi:10.2514/1.45733

[30] Williams, P., "Energy Rate Feedback for Libration Control of Electrodynamic Tethers," *Journal of Guidance, Control, and Dynamics*, Vol. 29, No. 1, 2006, pp. 221–223. doi:10.2514/1.17530

[31] Williams, P., "Libration Control of Electrodyanmic Tethers Using Predictive Control with Time-Delayed Feedback," *Journal of Guidance, Control, and Dynamics*, Vol. 32, No. 4, 2009, pp. 1254–1268. doi:10.2514/1.41039

[32] Iñarrea, M., and Peláez, J., "Libration Control of Electrodynamic Tethers Using the Extended Time-Delayed Autosynchronization Method," *Journal of Guidance, Control, and Dynamics*, Vol. 33, No. 3, 2010, pp. 923–933. doi:10.2514/1.44232

[33] Pizarro–Chong, A., and Misra, A. K., "Dynamics of Multi-Tethered Satellite Formations Containing a Parent Body," *Acta Astronautica*, Vol. 63, Nos. 11-12, 2008, pp. 1188–1202. doi:10.1016/j.actaastro.2008.06.021

[34] Zhaoa, J., and Cai, Z., "Nonlinear Dynamics and Simulation of Multi-Tethered Satellite Formations in Halo Orbits," *Acta Astronautica*, Vol. 63, Nos. 5–6, 2008, pp. 673–681. doi:10.1016/j.actaastro.2008.04.007

[35] Chung, S. J., "Nonlinear Control and Synchronization of Multiple Lagrangian Systems with Application to Tethered Formation Flight Spacecraft," Ph.D. Dissertation, Massachusetts Inst. of Technology, 2007.

[36] Kuramoto, Y., "Int. Symp. on Mathematical Problems in Theoretical Physics," edited by H. Arai, Springer, New York, Vol. 39, 1975, pp. 420–422.

[37] Vallado, D. A., "Fundamentals of Astrodynamics and Applications," 3rd ed., Microcosm Press, New York, 2007.